A Design Technique for Realizing a Microwave Tunnel-Diode Amplifier in Stripline

BARBARA A. MILLER, THOMAS P. MILES, MEMBER, IEEE, AND DONALD C. COX, MEMBER, IEEE

Abstract—**A significant problem in realizing a practical tunnel-diode amplifier is that of stabilizing the amplifier both within and outside its passband while maintaining a specified center-frequency gain and bandwidth. A new technique for realizing a moderate-bandwidth tunnel-diode amplifier that utilizes a directional filter as a bandpass structure is described.**

This technique was investigated analytically and an experimental *S*-band amplifier was built and tested. This experimental amplifier had typically the following characteristics: bandwidth, 400 MHz; center frequency, 2.9 GHz; and center-frequency gain, 12.5 dB.

The technique described yields an amplifier which is reproducible and which has an analytically predictable and well-defined response. None of the experimental models have shown any tendencies toward oscillations.

I. Introduction

A SIGNIFICANT PROBLEM in realizing a practical tunnel-diode amplifier is that of stabilizing the amplifier both within and outside its passband while maintaining a specified center-frequency gain and bandwidth. Most tunnel diodes are short-circuit as well as open-circuit unstable, and there is a range of resistive terminations that will terminate a given diode in a stable operating region. Hence, the impedance of the termination must be bounded over the entire active frequency range of the tunnel diode. Present-day circulators that maintain their characteristic impedance over an octave or more in frequency are not uncommon. However, the amplifier designer is still faced with the problem of providing the necessary termination outside the passband of the circulator, or in other words, isolating the tunnel diode from the circulator at these frequencies. One usual approach is to design frequency-selective loading circuits to stabilize the tunnel diode at frequencies lower and higher than the frequency range of the circulator.[1]–[3] Difficulties, such as oscillations and unpredictable responses, sometimes occur. This approach is appropriate when designing wideband as well as narrowband amplifiers.

A different and perhaps more straightforward technique for realizing a moderate-bandwidth tunnel-diode amplifier is described in this paper. This technique utilizes a directional filter as a bandpass structure. When properly terminated, a directional filter inherently maintains its input impedance both within and outside its passband and hence it conveniently lends itself to terminating a tunnel diode. The amplifier has a response which is determined to a first order by that of the directional filter. The resulting gains and noise figures are comparable with other design approaches. One inherent disadvantage of this approach is that the noise figure of the amplifier is somewhat degraded at the band edges. In addition, this design inherently yields stable amplifiers. Before discussing this specific amplifier, some general aspects of reflection-type tunnel-diode amplifiers shall be considered.

Manuscript received January 19, 1967; revised May 18, 1967. This work was supported by the USAF Avionics Lab. A portion of it was presented at the Internat'l Solid-State Circuits Conf., Philadelphia, Pa., February, 1965. It has also been published as a Stanford Electronics Labs. Rept., Stanford, Calif., March, 1966.

The authors are with the Systems Techniques Laboratory, Stanford Electronics Laboratories, Stanford, Calif.

II. Ideal Gain Equation for a Reflection-Type Amplifier

The gain equation for a reflection-type tunnel-diode amplifier will be derived in this section. Consider an ideal circulator connected to a transmission line which is terminated in an impedance $\overline{Z}_1$, as illustrated in Fig. 1(a).[1] If $\overline{Z}_1 \neq R_0$, then from transmission-line theory the reflection coefficient $\bar{\rho} = \overline{V}_{\text{ref}}/\overline{V}_{\text{in}}$ is determined by

$$\bar{\rho} = \frac{\overline{Z}_1 - R_0}{\overline{Z}_1 + R_0} = \frac{G_0 - \overline{Y}_1}{G_0 + \overline{Y}_1} \tag{1}$$

where $\overline{Y}_1 = 1/\overline{Z}_1$ and $G_0 = 1/R_0$. If the termination is a tunnel diode (that is, $\overline{Z}_1 = \overline{Z}_{TD}$ = tunnel-diode impedance) biased in its small-signal negative resistance region, then $|\overline{Z}_{TD} - R_0|$ may exceed $|\overline{Z}_{TD} + R_0|$ since the real part of $\overline{Z}_{TD}$ may be negative. Under these conditions $|\bar{\rho}|$ is greater than 1 and the circuit in Fig. 1(a) becomes an amplifier with gain $\overline{G}$ of

$$\overline{G} = \bar{\rho} = \frac{\overline{Z}_{TD} - R_0}{\overline{Z}_{TD} + R_0} = \frac{G_0 - \overline{Y}_{TD}}{G_0 + \overline{Y}_{TD}} . \tag{2}$$

For stable operation of the amplifier, R_0 must be chosen so that the gain expression has no poles in the right-half S plane. Stability criteria discussed by Hines[4] or by Henoch and Kvaerna[5] may be used to bound the value R_0. The exact value of R_0, within the stability rounds, may be chosen for convenience in using available hardware or may be determined by the desired amplifier gain response.

In a practical amplifier the ideal circulator can be replaced by an actual circulator if a constant-input impedance filter is placed in the line between the circulator and the tunnel diode as in Fig. 1(b). This filter will then limit the active bandwidth of the amplifier and maintain the diode termination at R_0 to insure stable operation. Since both the input signal and output (reflected) signal pass through the filter, it appears in the

[1] The bar notation over a capital letter indicates a complex number.

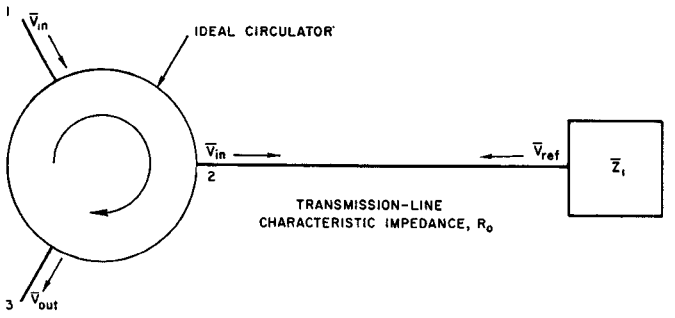

(a)

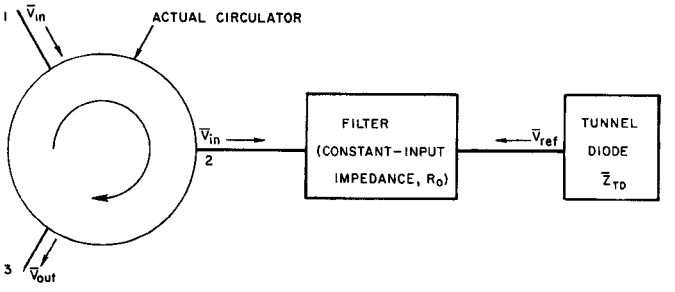

(b)

Fig. 1. Transmission-line models of tunnel-diode amplifiers. (a) Ideal reflection-type amplifier. Ideal circulator characteristics which hold for all frequencies, including dc, are as follows: 1) signals entering port 1 will exit port 2, 2) signals entering port 2 will exit port 3, 3) signals entering port 3 will be completely absorbed, and 4) no signal reflection will occur at any port used as an input port. (b) Tunnel-diode amplifier with filter.

signal path as two identical cascaded filters. The resulting gain equation is

$$\overline{A}' = \overline{H}_{12}{}^2\overline{G} = \overline{H}_{12}{}^2\left(\frac{\overline{Z}_{TD} - R_0}{\overline{Z}_{TD} + R_0}\right) \tag{3}$$

where $\overline{H}_{12}$ is the transfer characteristic of the filter. In Section III we will consider modifying $\overline{Z}_{TD}$ with compensating elements to produce a $\overline{G}$ which will yield a desired amplifier gain response $\overline{A}'$.

III. Compensation of a Tunnel Diode to Shape Amplifier Passband and Increase Amplifier Gain

To realize useful gains from tunnel diodes that have reasonably low cutoff frequencies, it is necessary to add frequency compensation between the tunnel diode and the filter. The determination of compensating element values for modifying the tunnel-diode impedance $\overline{Z}_{TD}$ will be discussed in this section using graphical techniques described by Henoch and Kvaerna.[3] To describe the method a specific tunnel diode is used. These techniques are applied to an amplifier with an ideal circulator and a reflectionless transmission line as shown in Fig. 2.

The requirement for an ideal circulator was removed in the preceding section by placing a constant input impedance filter between the compensating elements and an actual circulator. The effects of small reflections are dealt with in Section IV. The design method is based on modifying the tunnel-diode amplifier gain relation in (2).

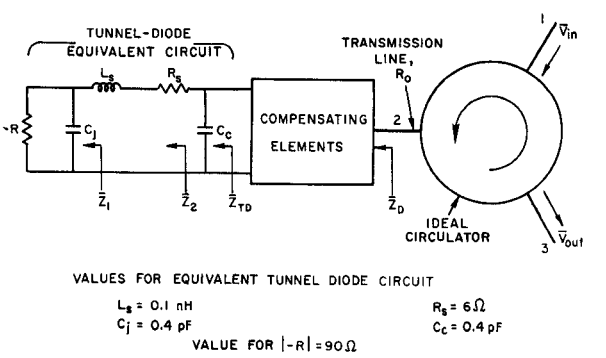

Fig. 2. Model of compensated ideal tunnel-diode amplifier.

The compensating elements have an effect on the amplifier similar to the effect produced by the tunnel-diode equivalent circuit elements which make up $\overline{Z}_{TD}$. Thus the gain of a compensated amplifier is given by the tunnel-diode gain equation, with $\overline{Z}_{TD}$ (the impedance of the tunnel diode) replaced with $\overline{Z}_D$ (the general expression for the impedance of the uncompensated or compensated tunnel diode); that is,

$$\overline{G} = \frac{\overline{Z}_D - R_0}{\overline{Z}_D + R_0} = \frac{G_0 - \overline{Y}_D}{G_0 + \overline{Y}_D}. \tag{4}$$

The design example was carried out using a commercially available diode which has the equivalent circuit values given in Fig. 2. Figure 3(a) shows the tunnel-diode equivalent circuit and one possible compensation network. The equivalent circuit terminated by an ideal resistance R_0 can be considered the uncompensated case. The frequency compensation network shown is the case of series-inductance compensation. Element values for compensation networks are determined graphically by forcing the complex impedance versus frequency plot of the compensated tunnel diode to conform closely to constant-gain circles, while continuing to satisfy the necessary stability criteria as discussed by Henoch and Kvaerna.[3],[5] For the simple case considered here, it is sufficient to require that the added series inductance does not cause the complex impedance plot of the series compensated tunnel diode to intersect the real axis to the left of $-R_0$ [Fig. 3(b)].

Figure 3(b) illustrates the technique used to determine the compensation element values. In this figure, negative reactance is plotted in the upward direction in the vertical axis; the horizontal scale is negative resistance to the left. A third grid is the constant-gain circles for gains ranging from +5 to +15 dB and for $R_0 = 50$ ohms. The solid plot is the impedance of the diode. The plot starts with zero frequency at −84 ohms and crosses the imaginary axis at its resistive cutoff frequency, which in this case is 16.5 GHz. Note that in the vicinity of 3 GHz the gain is approximately 6 dB. The dashed curve is for series-inductance compensation. The vertical displacement at any frequency from that of the uncompensated case is the added reactance. In this case 1.2 nH raised the gain to 10 dB at 3 GHz. For this particular amplifier a one element compensation network was sufficient. However, this general technique may be used to design more elaborate compensation networks.[6]

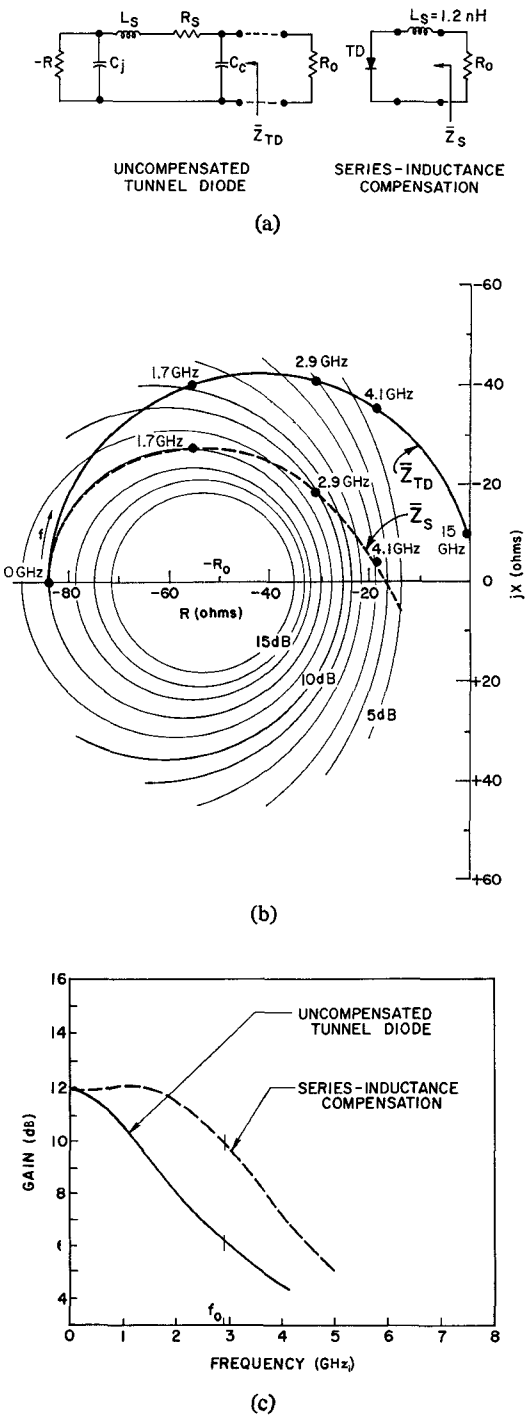

Fig. 3. Frequency compensation technique. (a) Frequency compensation networks. (b) Effects of compensation on complex impedance curves. (c) Effects of compensation on ideal amplifier response.

In Fig. 3(c) the information on the previous figure is replotted to emphasize the gain versus frequency response of the ideal amplifier. Again, the solid curve is for the uncompensated case and the dashed curve is the series-inductance compensation.

As previously mentioned, the overall passband response of the amplifier considered here will be determined in most part by that of the directional filter. However, frequency compensation is still necessary to obtain reasonable amplifier gains at microwave frequencies. The analysis, up to this point, has not considered the effects of small reflections which will certainly occur in a practical tunnel-diode amplifier.

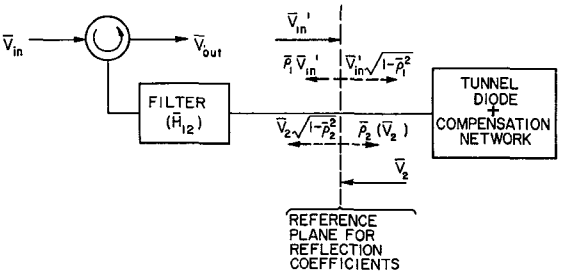

Fig. 4. Effects of small reflections.

IV. Effects of Small Reflections on Amplifier Gain

In this section the effects on amplifier gain of small reflections are considered. As shown in Fig. 4, all reflections resulting from both the filter and the circulator are referred to the characteristic impedance of the transmission system at a plane immediately preceding the compensation elements. The primary input wave $\overline{V}'_{in}$ breaks up into a transmitted wave $\overline{V}'_{in}\sqrt{1-\bar{\rho}_1^2}$ continuing on to the tunnel diode and a reflected wave $\bar{\rho}_1\overline{V}'_{in}$ traveling in the opposite direction. Similarly, the amplified wave $\overline{V}_2$ breaks up into a transmitted wave $\overline{V}_2\sqrt{1-\bar{\rho}_2^2}$ traveling on to the filter and a reflected wave $\bar{\rho}_2\overline{V}_2$ which travels back to the tunnel diode. For $|\bar{\rho}_1| \ll 1$, $|\bar{\rho}_2| \ll 1$, and $|\overline{G}| > 1$, the expression for the overall gain of the amplifier is

$$A \triangleq \frac{\overline{V}_{out}}{\overline{V}_{in}} \approx \overline{H}_{12}^2\left(\frac{\overline{G}}{1-\bar{\rho}_2\overline{G}}\right) \tag{5}$$

where $\overline{V}_{in}$ is the input to the circulator and $\overline{V}_{out}$ is the output of the circulator. (For derivation of (5) see the Appendix.)

When compared with (3) it can be seen that $\bar{\rho}_2$ behaves as a feedback term around the reflectionless amplifier. Since both $\bar{\rho}_2$ and $\overline{G}$ are complex, $\bar{\rho}_2$ can either raise or lower the gain of the amplifier. In the usual case $\bar{\rho}_2$ is due to random circuit discontinuities for which phase angle is not controlled. Therefore, in order for the overall gain $\overline{A}$ to correspond closely with the idealized response $\overline{A}' = \overline{H}_{12}^2\overline{G}$, a sufficient condition is that the $|\bar{\rho}_2|\,|\overline{G}|$ term must be small in comparison to 1. Finally, even though $\overline{G}$, the gain of the tunnel diode and compensation network, is stable, the total amplifier may be unstable because of the $(1-\bar{\rho}_2\overline{G})$ term. Instability can, however, be avoided by insuring that for all frequencies $|\bar{\rho}_2\overline{G}|$ is less than 1.

V. Amplifier Description and Directional-Filter Design

A. Amplifier Description

A directional filter composed of two quarter-wave directional couplers joined by a resonant loop is shown in Fig. 5(a). This directional filter is described more completely by Coale.[7] The response of the filter is illustrated in Fig.

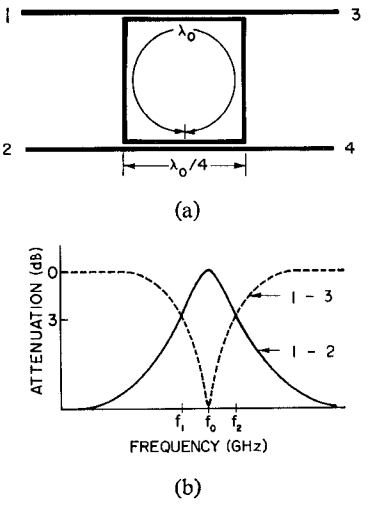

Fig. 5. Directional filter. (a) Configuration, (b) Idealized frequency response.

5(b). There is a bandpass response from ports 1 and 2 and a band-reject response from ports 1 and 3. Ideally no power would emerge from port 4. The filter is symmetrical and therefore any port could be considered the input. The electrical length of the resonant loop l specifies the center frequency, whereas the coupling coefficient of the directional couplers specifies the filter bandwidth, i.e., tighter coupling results in lower Q. The number of loops in the directional filter defines how many poles will be in the filter response; thus a single loop as shown here leads to a single-pole filter response. As a result of its directivity, the idealized input impedance at a given port is maintained at a constant R when the corresponding bandpass and band-reject ports are terminated inband and outband, respectively. This constant R characteristic thus provides a simple and straightforward means of terminating a tunnel diode.

The electrical configuration of the entire amplifier employing a directional filter is shown in Fig. 6. The tunnel diode is terminated within the amplifier passband by the circulator at port 1. Outside the passband, the tunnel diode is terminated by the broadband termination shown as part of the biasing network at port 4.

Now consider the signal flow of the amplifier. Input signals at frequencies within the filter bandwidth are coupled through the circulator to the tunnel diode by way of ports 1 and 2 of the filter. They are reflected with gain by the tunnel diode and coupled back to the circulator again through ports 2 to 1 of the filter. Signals within the circulator bandwidth but outside the bandwidth of the filter are absorbed in a termination at port 3. Since the filter appears twice in the signal path, a single-pole filter leads to a synchronous two-pole amplifier response.

The noise figure characteristic of this amplifier may be described by first considering the noise figure as measured at the tunnel diode. Here there are two contributions to the noise figure: 1) the thermal noise of the equivalent 50 ohm resistance, which terminates the tunnel diode at all frequencies due to the characteristics of the filter and 2) the excess noise of the tunnel diode.

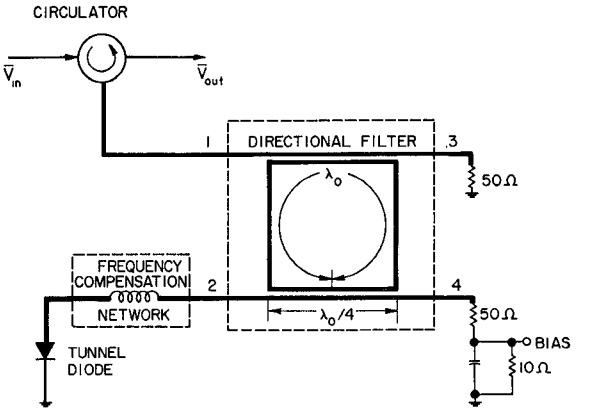

Fig. 6. Configuration of tunnel-diode amplifier.

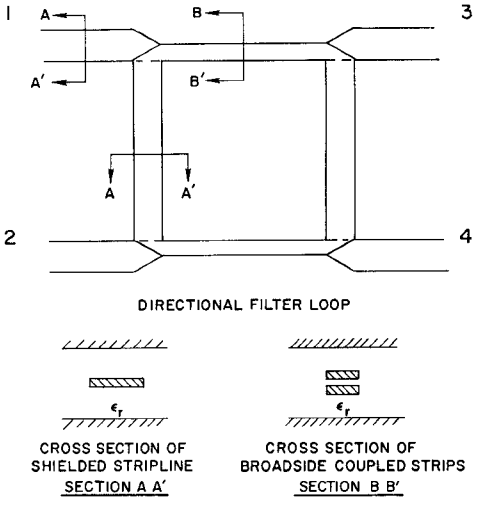

Fig. 7. Stripline configurations.

In referring the noise figure at the tunnel diode back to the input of the amplifier, it is increased by the circulator loss and the one-way filter attenuation. The loss associated with the circulator which was used is approximately 0.3 dB across the band. The filter attenuation is 0.2 dB at midband due to losses and 1.5 dB at the amplifier's 3 dB points. Although the noise figure as measured at the input is primarily due to the above considerations, there is one additional noise source which is negligible in most cases. A fraction of the thermal noise power generated by the resistor at port 3 will combine with the amplified signal plus noise as it leaves the amplifier. Since this noise power will be decreased by the gain of the amplifier when referring it back to the input of the amplifier, its contribution to the total noise figure is negligible.

The directional-filter and directional-coupler design equations are presented.[6],[8]–[10] The design criteria for the specific directional filter used in the experimental amplifier are: center frequency, $f_0 = 2.9$ GHz, and 3 dB bandwidth, BW = 700 MHz. (Using the bandwidth shrinkage factor $\sqrt{2^{1/n}-1}$ with $n=2$, a one-pole filter response with a bandwidth of 700 MHz corresponds to a two-pole amplifier response with a bandwidth of 450 MHz.) The geometry of the stripline, coupling region, and filter loop are presented in Fig. 7.

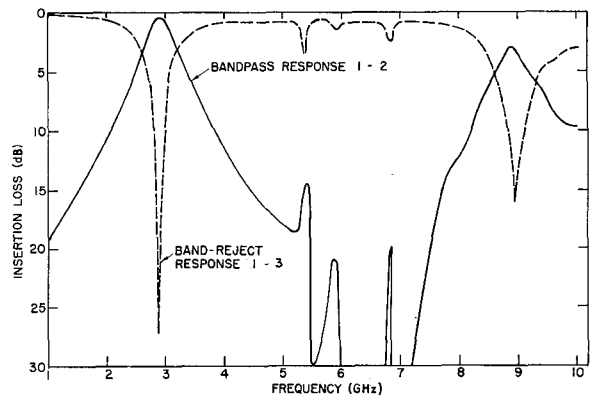

Fig. 8. Measured filter response.

The measured frequency response of one directional filter, which was subsequently used in the experimental amplifier, is shown in Fig. 8. The bandpass and band-reject responses are shown from 1 to 10 GHz. The fundamental response of this filter has a 3 dB bandwidth of 620 MHz centered at 2.9 GHz. The midband insertion loss is 0.5 dB. The response in the vicinity of 3.0 GHz is the only portion pertinent to the transmission of the amplifier being discussed, but it is necessary to consider the response at other frequencies for stability purposes. There are two spurious responses at 5.4 and 6.8 GHz which are cavity modes caused by the sidewalls in the stripline structure. The response at 5.9 GHz resulted because the electrical length of the loop was approximately two wavelengths long at this frequency. The response is very high Q since little power is coupled there. At 9.0 GHz the loop is approximately three wavelengths long. The response is low Q since there is tight coupling at the coupler's three-quarter wavelength frequency. At this frequency the midband insertion loss is 3.0 dB. Since the circulator does not provide a good match at this frequency, instability could occur if adequate gain were available from the tunnel diode. For the experimental amplifier discussed in this paper, the series-compensated tunnel diode had a gain of approximately 1.0 dB at this frequency. For this gain and the VSWR measured, the conditions for stability were satisfied.

VI. Experimental Tunnel-Diode Amplifier

The experimental tunnel-diode amplifier shown in Fig. 9 was constructed using stripline techniques. In the photograph a portion of the top cover plate has been removed to expose the stripline structure. In constructing this amplifier assembly an attempt was made to maintain as much control as possible over the various significant parameters and also to allow for measurements at intermediate stages of assembly. To provide for such measurements, the stripline structure was laid out in a manner which made it possible to gain access to various areas without disturbing adjacent circuitry. This was done, however, at the sacrifice of increased size. The stripline elements were etched from beryllium copper and subsequently laid on the tellite dielectric.

In Fig. 9 the principal components of the tunnel-diode amplifier are labeled. The circulator is located at port 1 of the directional filter. It was important that the circulator used be constructed in stripline with the same ground-plane spacing as the remainder of the amplifier; since then it was only necessary to transition the center conductors. Port 3 of the filter is terminated internally with a 50 ohm pill-type termination.

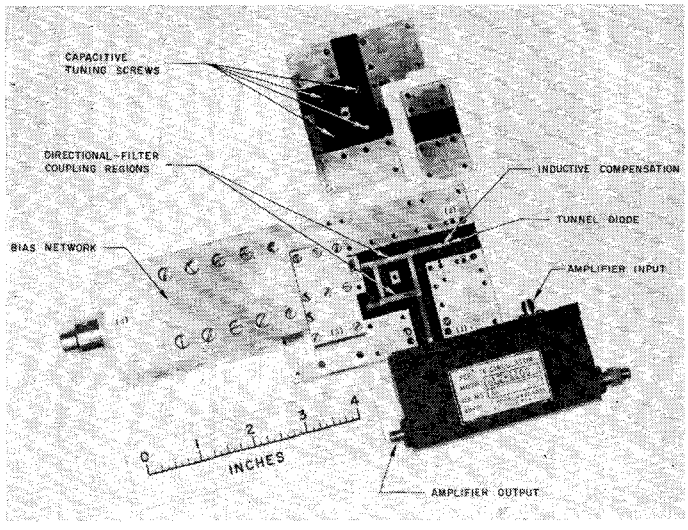

Fig. 9. Experimental tunnel-diode amplifier.

Four capacitive tuning screws are located in the top plate which covers the filter area. These tuning screws are used to compensate the inherently inductive corners of the filter.

The tunnel diode was mounted in the dielectric at port 2 of the directional filter. Inductive compensation was added by narrowing the center conductor immediately preceding the tunnel diode.

The bias network is mounted at port 4 of the filter. Its purposes are to provide a means of applying the tunnel-diode bias current and also to provide a stable termination for the tunnel diode. This termination should be resistive and have a value of approximately 50 ohms.

In assembling the amplifier, the characteristics of the directional filter were first measured with a connector at the tunnel-diode port. To reduce the level of reflections developed within the directional filter, the four tuning screws were adjusted for minimum inband voltage-reflection coefficient $|\bar{\rho}_2|$ looking into the diode port of the filter. The value of $|\bar{\rho}_2|$ inband is typically less than 5 percent.

After the filter was adjusted, the connector at the diode port was removed. A small corner of the cover plate was also removed to expose the area in which the tunnel diode was to be placed. The filter was not disturbed at or beyond this point of assembly. After the diode was inserted, the series inductance was adjusted to produce the desired midband amplifier gain.

The four-port circulator used in this amplifier made it unnecessary to have an impedance match at either the input or the output of the amplifier. With this arrangement it was a fairly simple task to minimize the inband voltage-reflection coefficient measured at the diode port to typically less than 5 percent, as shown in Fig. 10(a). Note also that for this

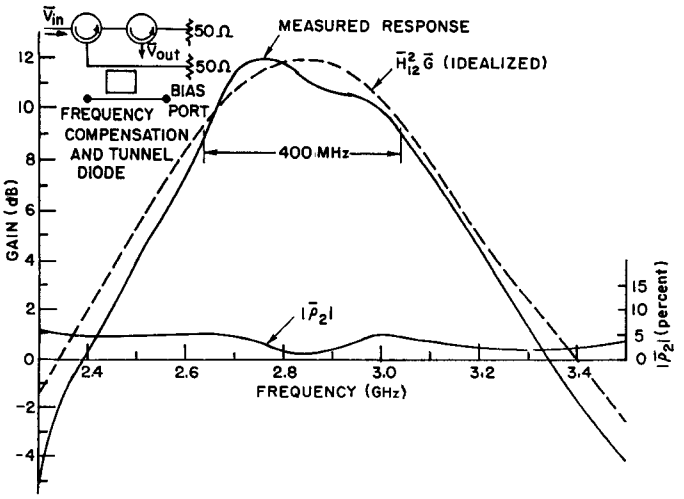

(a)

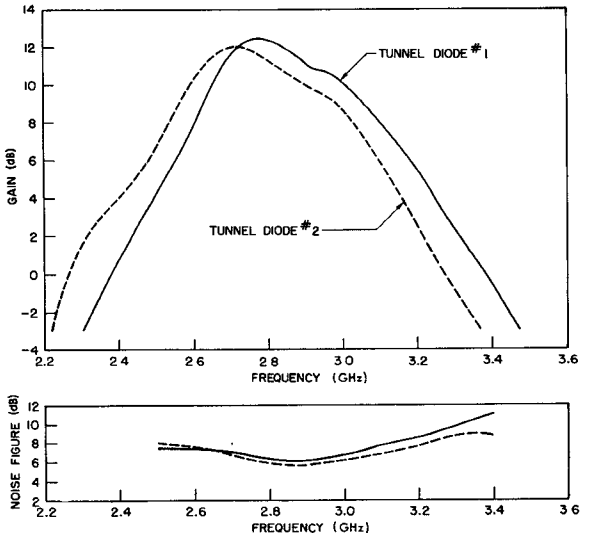

(b)

Fig. 10. Amplifier characteristics. (a) Frequency response of the tunnel-diode amplifier. (b) Effects on amplifier gain and noise figure resulting from the interchanging of diodes.

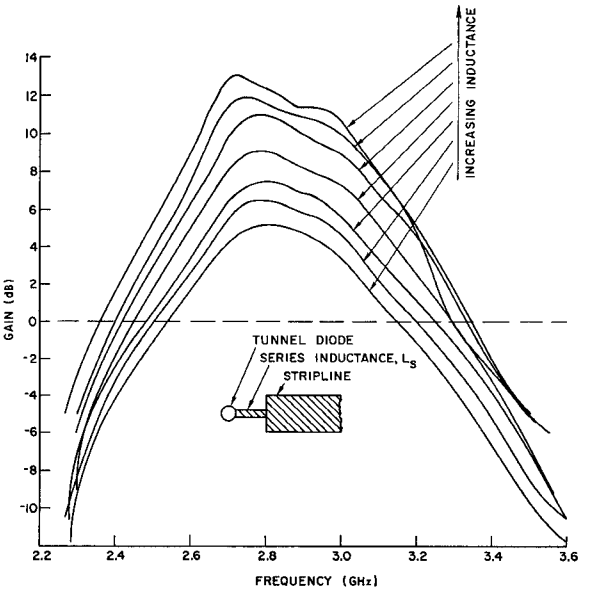

Fig. 11. Variation of amplifier gain response with increasing inductance.

amplifier the level of reflections is under 5 percent from 2.3 to 3.5 GHz. The effects of $\bar{\rho}_2$ on the amplifier response may be noted from this figure by comparing the measured response to the idealized response, $\overline{H}_{12}{}^2\overline{G}$. For a gain of 12 dB and a 5 percent reflection level, one can expect a maximum deviation of ± 2 dB between the actual and the ideal response. In this case the deviation near midband was only slightly greater than ± 1 dB.

Gain and noise-figure measurements were conducted on the tunnel-diode amplifier using two different tunnel diodes. These measurements are shown in Fig. 10(b). The diodes were simply interchanged without retuning or varying the inductance compensation. The shift of the center frequency is probably due to a difference in the lowpass characteristic of the two tunnel diodes with compensation. The noise-figure measurements verified that the general shape of the noise figure versus frequency curve for the amplifier followed very closely that of a single-pole filter. In other words, the noise figure can be expected to be a minimum at the center frequency of the filter and 1.5 dB higher at the 3 dB band edges of the two-pole filter response, which are also approximately those of the amplifier. The calculated midband noise figure of the amplifier, based on diode parameters and including both circulator and filter losses, was 5.2 dB. The difference between the measured and calculated values was well within the measurement error of the system. The similarity of the gain and noise figure as functions of frequency for the two diodes seems to indicate that the basic design is, as expected, relatively insensitive to the diode parameters.

In order to verify experimentally a portion of the analytical work pertaining to the compensation networks, the amplifier gain response was measured for various values of series-inductance compensation. The inductance was varied by adjusting the width of the stripline center conductor immediately preceding the tunnel diode. The experimental gain responses are shown in Fig. 11. There are certain trends due to increasing inductance which can be noted from these curves and which agree closely with those predicted analytically using a complex impedance plot. First, the gain at the frequency corresponding to the uncompensated amplifier center frequency increases with increasing inductance. If the value of inductance were increased even further, a value would be reached whereupon this center frequency gain would begin to decrease. Second, there is a downward shift in frequency of the maximum amplifier gain. Another trend evident in these curves and which is analytically predictable is the increasing distortion of the gain response from the ideal reflectionless response with increasing magnitudes of gain. Comparison of (3) and (5) indicates that the effect of reflections on the gain response becomes greater with increasing gain and causes the actual response to differ more and more from the ideal. It was predicted from the

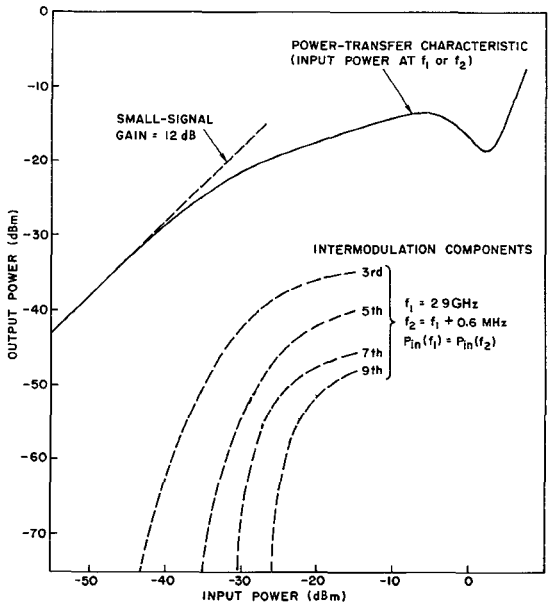

Fig. 12. Center-frequency power-transfer characteristics and intermodulation components of the tunnel-diode amplifier.

complex impedance plot that a gain of 11.5 dB (which includes filter and circulator losses of 1 dB) will occur at a center frequency of 2.9 GHz when a series inductance of 2.2 nH is used. The calculated value of inductance for the strip which experimentally yielded a gain of 11.5 dB is approximately 1.7 nH.

The output versus input power-transfer characteristic of the amplifier for input signals up to 7.5 dBm is shown in Fig. 12. The cause of the dip in the curve in the region of 0 dBm, a phenomenon which has been noted in similar devices, has not been analytically determined. The measured third- through ninth-order intermodulation components are also shown in Fig. 12.

VII. Conclusions and Discussion

This paper has presented a technique for realizing a tunnel-diode amplifier utilizing a directional filter. This technique was investigated analytically, and several experimental *S*-band amplifiers were built and tested. In general, the experimental results agree well with the predicted results.

In order to realize useful gains from diodes with moderate cutoff frequencies, compensation of the tunnel diode proved to be valuable. Since the amplifier was narrowband, simple forms of compensation were adequate. The graphical technique presented is a valuable tool in designing compensation networks for a reflection-type amplifier. Its usefulness is based on the fact that once the input impedance of the tunnel diode is plotted, the gain is immediately available from a grid of constant-gain circles for a given characteristic network impedance R_0. The network impedance can then be conveniently manipulated by the addition of compensating elements to give a desired gain response.

The experimental amplifier discussed in this report utilizes a single-pole filter which yields a two-pole amplifier. To extend this technique to the design of amplifiers with more than two poles, it would appear more desirable to cascade two-pole amplifiers rather than utilize multipole filters. This preference for cascaded amplifiers is partially based on the increased isolation that occurs when circulators are placed between the filters.

This method of realizing a tunnel-diode amplifier was demonstrated in *S* band. The use of this technique for higher frequency ranges is limited to the extent of realizing the filter and other components with adequately low reflection levels. The extension to lower frequency ranges is limited by size, since distributed instead of lumped elements would be used.

The amplifier's noise figure is degraded over the no-loss case only by the insertion loss of the filter, which is 0.4 dB at midband and which has the curvature of a single-pole filter response.

The technique in this paper yields an amplifier which is reproducible and which has a predictable and well-defined response. To date, none of the experimental models have shown any tendencies toward oscillations.

Appendix

Derivation of Actual Amplifier Gain Expression

The overall gain expression for the amplifier (see Fig. 4) is defined as

$$\overline{A} \triangleq \frac{\overline{V}_{out}}{\overline{V}_{in}} \tag{6}$$

where $\overline{V}_{in}$ is the input to the circulator and $\overline{V}_{out}$ is the output of the circulator. Now proceed with the derivation by defining

$$\overline{V}_1 = \sqrt{1-\bar{\rho}_1^2}\,\overline{V}'_{in} + \bar{\rho}_2\overline{V}_2. \tag{7}$$

For $|\bar{\rho}_1| \ll 1$, $\sqrt{1-\bar{\rho}_1^2}$ is approximately equal to 1, and therefore the expression for $\overline{V}_1$ becomes

$$\overline{V}_1 \approx \overline{V}'_{in} + \bar{\rho}_2\overline{V}_2. \tag{8}$$

Next solve for $\overline{V}_{in} = \overline{V}'_{in}/\overline{H}_{12}$, where $\overline{H}_{12}$ is defined as the filter transfer function.

$$\overline{V}_{in} = \frac{\overline{V}_1 - \bar{\rho}_2\overline{V}_2}{\overline{H}_{12}} = \frac{\overline{V}_1(1-\bar{\rho}_2\overline{G})}{\overline{H}_{12}} \tag{9}$$

where $\overline{G} = \overline{V}_2/\overline{V}_1$. The circulator output $\overline{V}_{out}$ is given by

$$\overline{V}_{out} = \overline{H}_{12}[\sqrt{1-\bar{\rho}_2^2}\,\overline{V}_2 + \bar{\rho}_1\overline{V}'_{in}]. \tag{10}$$

For $|\bar{\rho}_2| \ll 1$, $\sqrt{1-\bar{\rho}_2^2}$ is approximately equal to 1, and for $|\bar{\rho}_1| \ll 1$ and $|\overline{G}| > 1$, the reflected portion of the input wave $\bar{\rho}_1\overline{V}'_{in}$ is small compared to $\overline{V}_2 = \overline{G}\overline{V}_1$ and can be neglected. The expression for $\overline{V}_{out}$ becomes

$$\overline{V}_{out} \approx \overline{H}_{12}\overline{V}_2 = \overline{H}_{12}\overline{G}\overline{V}_1. \tag{11}$$

Finally, the expression for the overall gain of the amplifier is found to be

$$\overline{A} \triangleq \frac{\overline{V}_{out}}{\overline{V}_{in}} \approx \overline{H}_{12}^2\left(\frac{\overline{G}}{1-\bar{\rho}_2\overline{G}}\right). \tag{12}$$

References

[1] J. Hamasaki, "A low-noise and wide-band Esaki diode amplifier with a comparatively high negative conductance diode at 1.3 Gcs," *IEEE Trans. Microwave Theory and Techniques*, vol. MTT-13, pp. 213–223, March 1965.

[2] J. O. Scanlan and J. T. Lim, "The effect of parasitic elements on reflection type tunnel diode amplifier performance," *IEEE Trans. Microwave Theory and Techniques*, vol. MTT-13, pp. 827–836, November 1965.

[3] B. T. Henoch and Y. Kvaerna, "Broadband tunnel-diode amplifiers," Stanford Electronics Labs., Stanford, Calif., Rept. SEL-62-099 (TR213-2), AD 299 284, August 1962.

[4] M. E. Hines, "High-frequency negative-resistance circuit principles for Esaki diode applications," *Bell Sys. Tech. J.*, pp. 477–513, May 1960.

[5] B. Henoch and Y. Kvaerna, "Stability criteria for tunnel-diode amplifiers," *IRE Trans. Microwave Theory and Techniques* (*Correspondence*), vol. MTT-10, pp. 397–398, September 1962.

[6] B. A. Miller, T. P. Miles, and D. C. Cox, "A design technique for realizing a microwave tunnel-diode amplifier in stripline," Stanford Electronics Labs., Stanford, Calif., Rept. SU-SEL-66-022 (TR1973-1), March 1966.

[7] F. S. Coale, "A traveling-wave directional filter," *IRE Trans. Microwave Theory and Techniques*, vol. MTT-4, pp. 256–260, October 1956.

[8] S. B. Cohn *et al.*, "Research on design criteria for microwave filters," Stanford Research Inst., Menlo Park, Calif., Final Rept., SRI Project 1331, Contract DA36(039) SC-64625, AD 157 528, June 1957.

[9] S. B. Cohn *et al.*, "Strip transmission lines and components," Stanford Research Inst., Menlo Park, Calif., Final Rept. SRI Project 1114, Contract DA36(039) SC-63232, AD 145 251, February 1957.

[10] G. L. Matthaei *et al.*, "Design criteria for microwave filters and coupling structures," Stanford Research Inst., Menlo Park, Calif., Final Rept. SRI Project 2326, Contract DA36(039) SC-74862, AD 255 509, January 1961.

The Overdriven Varactor Upper Sideband Upconverter

ALFRED I. GRAYZEL, MEMBER, IEEE

Abstract—**The equations for the overdriven upper sideband upconverter are derived and computer solutions are given for the abrupt junction, graded junction, and punch through varactor. The necessary design parameters are presented for the design of an upconverter. The performance of the abrupt, graded, and punch through varactors are compared.**

List of Symbols

$C(V)$ = Junction capacitance as a function of voltage across it in the reverse direction

Eff = Efficiency—power out divided by total power in

$f_c(V)$ = Cutoff frequency [defined by (16)] as a function of V

P_K = Total power into varactor for $K=1$, and 2 and out of varactor for $K=3$ [see (12)]

P_{0K} = The power into the lossless varactor at frequency ω_K ($K=1, 2, 3$)

P_{DK} = The power dissipated in R_s at frequency ω_K ($K=1, 2, 3$)

q = The charge on the varactor

$\bar{q}$ = The normalized charge defined by (2)

q_ϕ = The charge due to the contact potential

Q_0 = Average normalized charge on the varactor

$\overline{Q}_K$ = Normalized charge on varactor at frequency ω_K ($K=1, 2, 3$) defined by (4)

Q_B = Charge at breakdown

R_K = Real part of "impedances" (ratio of voltage to current) across the varactor at ω_K

$\overline{R}_K$ = Normalized resistance defined by (19)

R_S = Parasitic series resistance of diode

$S_{\max}$ = Maximum value of the varactor elastance—value of elastance at breakdown

T = Period of charge waveform

V_B = Breakdown voltage

V = Voltage across lossless varactor in reverse direction

$\overline{V}$ = Normalized voltage across varactor defined by (2)

$\overline{V}_{KC}$ = Voltage across diode at frequency ω_K in phase with the current at ω_K

$\overline{V}_{KS}$ = Voltage across diode at frequency ω_K out of phase with current at ω_K

V_0 = dc voltage across varactor

$\overline{V}_0$ = Normalized dc voltage across varactor

X = Parameter in (15)

X_K = Imaginary part of "impedances" (ratio of voltage to current) across the varactor at ω_K

$\overline{X}_K$ = Normalized imaginary part of the impedance defined by (19)

α = Loss coefficient defined by (17)

β = Normalized output power defined by (18)

γ = Varactor law defined by (1)

ϕ = Contact potential

$\omega_1 = 2\pi$ times the input frequency

$\omega_2 = 2\pi$ times the pump frequency

$\omega_3 = 2\pi$ times the output frequency

$\omega_c = 2\pi$ times $f_c(V_B)$

θ_K = The phase angle of the charge waveform at ω_K for $K=2$ and 3 in (4)

Manuscript received January 16, 1967; revised May 16, 1967.

The author was formerly with the M.I.T. Lincoln Laboratories, Lexington, Mass. He is presently with NASA-Electronics Research Center, Cambridge, Mass.